Scaling of Decoherence in Wide NMR Quantum Registers

Hans Georg Krojanski and Dieter Suter
Universität Dortmund, Fachbereich Physik, 44221 Dortmund, Germany
(Received 31 March 2004; published 24 August 2004)

Among the most important parameters for the usefulness of quantum computers are the size of the quantum register and the decoherence time for the quantum information. The decoherence time is expected to get shorter with the number of correlated qubits, but experimental data are only available for small numbers of qubits. Solid-state nuclear magnetic resonance allows one to correlate large numbers of qubits (several hundred) and measure their decoherence rates. We use a modified magnetic dipole-dipole interaction to correlate the proton spins in a solid sample and observe the decay of the resulting highly correlated states. By systematically varying the number of correlated spins, we measure the increase of the decoherence rate with the size of the quantum register.

DOI: 10.1103/PhysRevLett.93.090501 PACS numbers: 03.67.Pp, 03.65.Yz, 03.67.Lx, 82.56.Hg

Quantum information processing holds enormous potential for some problems that cannot be solved efficiently on classical computers. The most successful experimental demonstrations of quantum computing so far were based on liquid-state nuclear magnetic resonance (NMR), where Shor's algorithm was implemented on a 7-qubit quantum computer [1], and on trapped ions, where a 2-qubit Deutsch-Jozsa algorithm was realized [2]. First prototypes of solid-state systems have also been demonstrated (see, e.g., [3,4]). For these (and some other) systems, solutions have been found (or proposed) to fulfill the basic requirements for the physical implementation of quantum computing [5]. However, to become useful, all of these systems must be scaled to significantly larger numbers of qubits. Possibly the largest obstacle to such an increase in the number of qubits will be the decoherence, which is expected to be faster in larger systems. To achieve reliable operation of a quantum computer, it must be possible to perform thousands of gate operations before decoherence has destroyed the quantum information [6].

For most proposed systems, figures of merit for these numbers have been estimated (see, e. g. [7]). So far, all these estimates are based on decoherence times that are measured (if available) or estimated for *individual* qubits. During any quantum algorithm, however, the information that is stored in the quantum register is not localized in individual qubits, but distributed over the whole quantum register. Most of the relevant states involve correlations and entanglement among a large number of (sometimes all) qubits present in the system. It is generally expected that the decoherence of such highly correlated states will be faster than that of individual qubits. Up to now no detailed theoretical predictions exist and no experimental results are available that verify this behavior. The most detailed experimental data available so far are from NMR, where relaxation rates of individual spins are routinely measured in liquids as well as in solids. For many of these systems, relaxation rates can also be calculated with high precision. However, with few exceptions experimental as well as theoretical work has been restricted to uncorrelated spins. Only a few experimental data are available for correlated states of two-spin systems [8,9] and no experimental data exist about the decay of large clusters of correlated spins.

In this Letter, we measure the decoherence rate for highly correlated spin states and present initial data on the scaling of the decoherence rate with the number of correlated spins. While several schemes have been proposed for scalable implementations of quantum information processing on the basis of spins in solids [10–12], these systems are not yet sufficiently advanced to perform such measurements. On the other hand, for the measurement of decoherence rates, the system does not have to fulfill all the requirements that a real quantum computer must satisfy. In particular, we can drop the requirements of individual addressing of qubits for excitation as well as for detection. This allows us to use solid-state nuclear spins as qubits, which can be correlated through their magnetic dipole-dipole interaction. We then measure the decoherence rates of correlated spin clusters consisting of

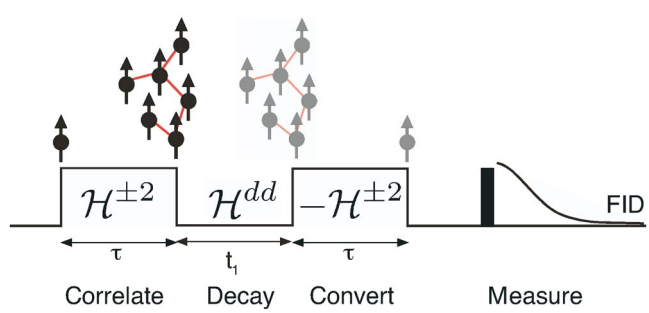

FIG. 1 (color online). Experimental scheme: The effective Hamiltonian $\mathcal{H}^{\pm 2}$ creates correlations between the spin qubits. During t_1, these coherences decay. The conversion step transfers the coherence amplitudes into observable magnetization, and the readout measures them as the amplitude of the FID.

up to 650 spins as a function of their size using solid-state NMR multiple pulse techniques.

The measurements were performed on a system of nuclear spins $I = 1/2$. In thermal equilibrium, its density operator can be written as [13]

$$\rho_{eq} = \mathbf{1} + \alpha \sum_i I_z^i, \tag{1}$$

where the I_z^i are the z components of the spin operators and α is a temperature-dependent numerical constant on the order of 10^{-5}. The individual spins are thus uncorrelated and their relaxation is independent of each other.

As shown in Fig. 1, we create the highly correlated spin states by letting the spin system evolve under a Hamiltonian of the form

$$\mathcal{H}^{\pm 2} = -\frac{1}{2} \sum_{j,k} d_{jk} [I_+^j I_+^k + I_-^j I_-^k], \tag{2}$$

where d_{jk} is the dipole-dipole coupling constant and the sum runs over all spins in the sample. Under the effect of this Hamiltonian, the initial equilibrium spin state evolves into

$$\rho(\tau) = e^{-i\mathcal{H}^{\pm 2}\tau} \rho_{eq} e^{i\mathcal{H}^{\pm 2}\tau} = \sum_{LMK} a_{LMK} \mathbf{A}_{LMK}. \tag{3}$$

Here we expand the density operator in terms of irreducible tensor operators $\mathbf{A}_{LMK}$, where L, M are the rank and order of the tensor operator, while K refers to the number of correlated spins for the specific operator. Additional quantum numbers, which would be required for complete labeling, have been omitted for clarity. The individual operators can also be written as products of spin operators $\mathbf{A}_{LMK} = \sum_\alpha c_\alpha I_+^i I_-^k I_z^l \ldots$. As we show below, the experiment creates measurable amounts of such correlated spin clusters with several hundred spins.

After the creation of these states, we let them decay under the influence of dipole-dipole couplings, which can be represented by the Hamiltonian

$$\mathcal{H}^{dd} = \sum_{j,k} d_{jk} [3 I_z^j I_z^k - \vec{I}^j \vec{I}^k]. \tag{4}$$

Our experiment measures the decay of the coherence amplitudes a_{LMK}. We write this decay in the form

$$a_{LMK}(t_1) = a_{LMK}(0) f_{LMK}(t_1), \tag{5}$$

where $f_{LMK}(t_1)$ is the decay function in which we are interested.

Since the operators $\mathbf{A}_{LMK}$ are not directly observable, we transfer the amplitudes $a_{LMK}(t_1)$, whose decay we want to measure, into observable single spin magnetization. This can be achieved by an evolution under the operator

$$-\mathcal{H}^{\pm 2} = e^{-i(\pi/2)I_z} \mathcal{H}^{\pm 2} e^{i(\pi/2)I_z}, \qquad I_z = \sum_i I_z^i$$

Both operators $\pm\mathcal{H}^{\pm 2}$ are created as effective Hamiltonians by a multiple pulse sequence that is applied to the spin system [14].

After this conversion step, the nuclear spin polarization, which now contains the information about the coherence amplitudes, can be measured by applying a resonant radio frequency pulse that converts the longitudinal into transverse magnetization, and then measuring the free induction decay (FID). The amplitude of the FID is proportional to

$$s_{\mathrm{FID}}(t_1) \propto \sum_{LMK} |a_{LMK}(0)|^2 f_{LMK}(t_1). \tag{6}$$

The decay of the coherence is traced out by repeating the experiment for a sequence of decay times t_1.

Experiments were performed on a home-built solid-state NMR spectrometer operating at a ^1H resonance frequency of 360 MHz. For the spin system we used the protons of a powdered adamantane sample. Figure 2 shows the observed signal as a function of the time t_1. The different data sets connected by lines correspond to different pumping times τ, as indicated by the legend in the figure. The data show clearly that the decoherence gets faster as the pumping time gets longer and the number of correlated spins increases. For comparison, the figure also includes the free induction decay signal (solid line), which corresponds to the decay of uncorrelated spins. All of the highly correlated states are more fragile than the uncorrelated qubits that are usually taken as the reference.

In Fig. 2, the different data sets are labeled with the average number $\bar{K}$ of correlated spins (qubits) that contribute to the signal. To determine the average cluster size, we used the technique developed by Baum et al. [14]: We separated the different signal contributions to Eq. (6)

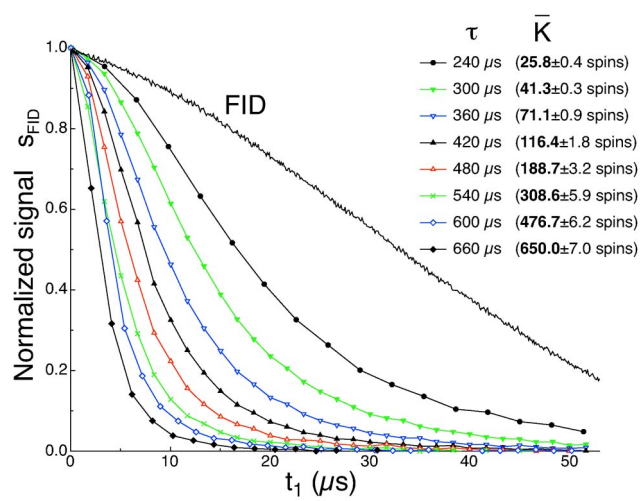

FIG. 2 (color online). Decay of coherence from highly correlated spin states. The different data sets represent different cluster sizes.

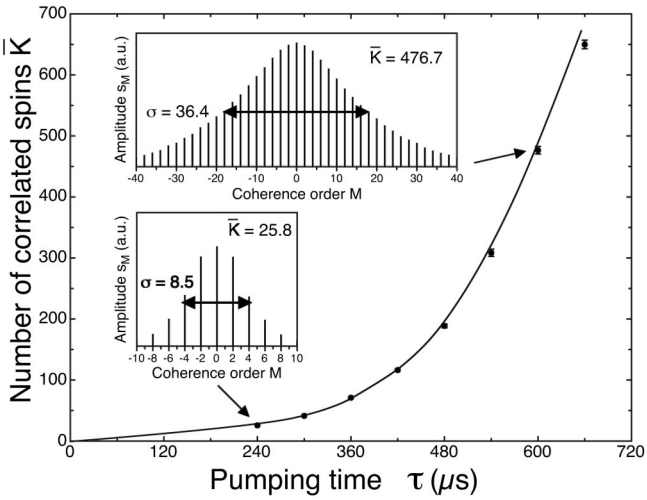

FIG. 3. Size $\bar{K}$ of the effective quantum register as a function of the pumping time τ. The points represent experimental values; the solid line is a guide to the eye. The two insets show examples of the distribution of signal into different coherence orders with half-width σ.

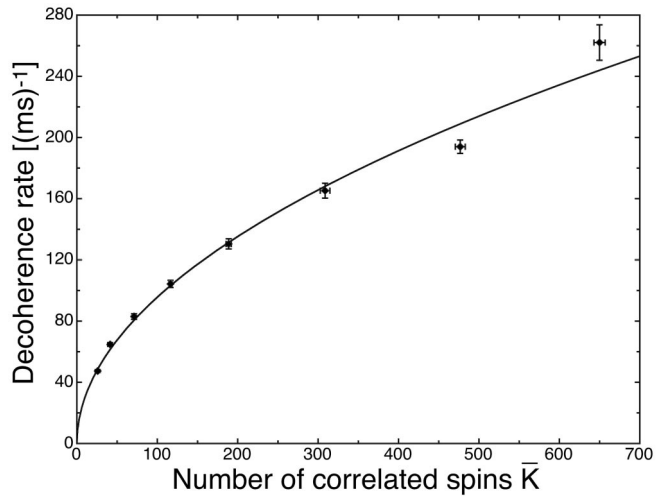

FIG. 4. Increase of the decoherence rate for increasing size of the spin clusters.

according to the coherence order M. For this purpose, we incremented the phase of the preparation pulse sequence systematically. This results in phase shifts of the individual coherences that are proportional to the coherence order M:

$$a_{LMK}(\phi) = e^{iM\phi} a_{LMK}(0). \tag{7}$$

The radio frequency phase ϕ was incremented and the measured signal was Fourier transformed with respect to ϕ to separate the signal contributions with different M.

Two of the distributions observed in this way are shown in Fig. 3 as insets. Comparison shows that for the longer pumping time ($\tau_2 = 600$ μs vs $\tau_1 = 240$ μs) the distribution has become wider, with significantly higher order coherences becoming excited. The cluster size can be determined from the assumption that the different coherence orders are excited with the same probability [14], i.e. that the observed dependence of the signal amplitude is directly proportional to the number of operators with the given coherence order, $n(K, M) = \frac{(2K)!}{(K+M)!(K-M)!}$. For large K, the distribution approaches a Gaussian,

$$n(K, M) \rightarrow 4^K (K\pi)^{-1/2} e^{-M^2/K}, \tag{8}$$

with half-width $\sigma = 2\sqrt{\ln 2 K}$. Fitting the signal amplitude of each coherence order, $s_M \propto \sum_{LK} |a_{LMK}(0)|^2$, against the coherence order M, we obtain the cluster size from the width σ of the distribution. As Fig. 3 shows, we found that the number of correlated spins increases rapidly with the duration of the pumping time.

The dependence of the decoherence rate on the number of correlated spins was obtained by repeating the measurements shown in Fig. 2 for increasing pumping times τ. For each pumping time, we determined the average cluster size as described above and measured the decoherence rates as the inverse of the $1/e$ decay time. Figure 4 shows the observed decoherence rates as a function of the number of correlated spins. As expected, the decoherence rates increase with increasing cluster size. The solid line, which is a fit to the function $y = B\sqrt{x}$, is meant to guide the eye.

The separation of the signal into different coherence orders also allows us to measure the decay of the different coherence orders individually. In Fig. 5, we compare the decay rates of the various coherence orders for different cluster sizes. Since the pumping Hamiltonian of Eq. (2)

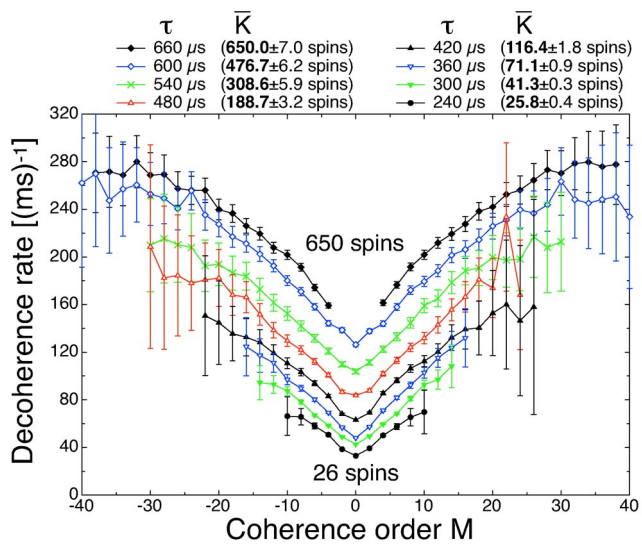

FIG. 5 (color online). Decoherence rates for different coherence orders and different cluster sizes.

contains only ± 2 quantum operators, the resulting spin state contains only even order coherences. For these, we analyzed the individual decay curves and determined decoherence rates as above.

As Fig. 5 shows, the decay becomes faster with increasing coherence order M. The behavior can be rationalized by noting that each K-spin cluster contributes only to signal components of order $M \leq K$. Higher order coherences contain therefore higher signal contributions from larger clusters, which are expected to decay faster. More detailed characterization of the decay rates for individual spin operators is possible by rotating the system around two orthogonal axes [15]. While such an approach would provide more detailed information about the spread of the individual decoherence rates, the successful implementation of quantum computing depends only on the average decay rate: During the execution of a quantum algorithm, the information is repeatedly spread over almost the full accessible Hilbert space. The resulting information will therefore decay not at the decay rate of an individual coherence, but at an average decoherence rate[16].

The experimental results presented here clearly demonstrate the expected increase of the decoherence rate with the number of correlated spins. This is in qualitative agreement with the behavior that is expected for increasing size of the number of qubits in a quantum register. The increase that we observed in this case is clearly less than linear in the number of qubits (see Fig. 4). If such a behavior can be verified in different systems, it raises the prospect for successful implementations of large-scale quantum computers, which hinges primarily on the relation between the decoherence rate and gate operation time. A linear increase of the decoherence rate with the number of qubits would be expected if the perturbations acting on the different qubits were completely uncorrelated. The slower increase therefore indicates that the perturbations are correlated. Some degree of correlation should be present in all physical systems that have been considered for the implementation of quantum information processing. It will be interesting to check if the observed proportionality of the decoherence rate to the square root of the cluster size can be rationalized, e.g., by statistical arguments or from scaling arguments involving the size of the cluster vs the average interaction with its environment. We plan to address these issues experimentally by varying the type of couplings and, possibly, the effective geometry of the clusters. As discussed before, the scaling behavior can be optimized by appropriately storing the quantum information in subspaces of the Hilbert space [16].

In the present system, the interaction between system and environment is non-Markovian, as the clearly non-exponential decay of the coherences shows. This is consistent with different models of decoherence, such as the spin-Boson model, over a wide parameter range [17]. In useful quantum computers, we expect that the coupling to the environment will be weak and the overall behavior should be well approximated by a Markovian process. We therefore plan to investigate the decay process with different types of interactions. This should be possible, in principle, in solid-state NMR, where we can use multiple pulse sequences to engineer suitable system-environment interactions.

The authors thank Dr. Marcus Eickhoff for technical support. Financial assistance was provided by the Deutsche Forschungsgemeinschaft through the Graduiertenkolleg 726.

[1] L. M. K. Vandersypen, M. Steffen, G. Breyta, C. S. Yannoni, M. H. Sherwood, and I. L. Chuang, Nature (London) **414**, 883 (2001).
[2] S. Gulde, M. Riebe, G. P. T. Lancaster, C. Becher, J. Eschner, H. Häffner, F. Schmidt-Kaler, I. L. Chuang, and R. Blatt, Nature (London) **421**, 48 (2003).
[3] I. Chiorescu, Y. Nakamura, C. J. P. M. Harmans, and J. E. Mooij, Science **299**, 1869 (2003).
[4] P. Bianucci, A. Muller, C. K. Shih, Q. Q. Wang, Q. K. Xue, and C. Piermarocchi, Phys. Rev. B **69**, 161303(R) (2004).
[5] D. P. DiVincenzo, Fortschr. Phys. **48**, 771 (2000).
[6] J. Preskill, Proc. R. Soc. London A **454**, 385 (1998).
[7] Quantum information science and technology roadmapping project, http://qist.lanl.gov/.
[8] A. Wokaun and R. R. Ernst, Mol. Phys. **36**, 317 (1978).
[9] K. Pervushin, R. Riek, G. Wider, and K. Wüthrich, Proc. Natl. Acad. Sci. U.S.A. **94**, 12366 (1997).
[10] B. Kane, Nature (London) **393**, 133 (1998).
[11] R. Vrijen, E. Yablonovitch, K. Wang, H.W. Jiang, A. Balandin, V. Roychowdhury, T. Mor, and D. DiVincenzo, Phys. Rev. A **62**, 012306 (2000).
[12] D. Suter and K. Lim, Phys. Rev. A **65**, 052309 (2002).
[13] A. Abragam, *The Principles of Nuclear Magnetism* (Oxford University Press, Oxford, 1961).
[14] J. Baum, M. Munowitz, A. Garroway, and A. Pines, J. Chem. Phys. **83**, 2015 (1985).
[15] D. Suter and J. Pearson, Chem. Phys. Lett. **144**, 328 (1988).
[16] C. S. Maierle and D. Suter, in *Quantum Information Processing*, edited by G. Leuchs and T. Beth (Wiley-VCH, Weinheim, 2003), p. 121.
[17] G. M. Palma, K.-A. Suominen, and A. K. Ekert, Proc. R. Soc. London A **452**, 567 (1996).